Pharmaceutical Research, Vol. 22, No. 5, May 2005 (© 2005)
DOI: 10.1007/s11095-005-2599-2

Research Paper

Surface Energy and Interparticle Force Correlation in Model pMDI Formulations

Daniela Traini,[1] Philippe Rogueda,[2] Paul Young,[1] and Robert Price[1,3]

Received November 1, 2004; accepted February 9, 2005

Purpose. To compare experimental measurements of particle cohesion and adhesion forces in a model propellant with theoretical measurements of the interfacial free energy of particulate interactions; with the aim of characterizing suspension stability of pressurized metered dose inhalers (pMDIs).
Methods. Interparticulate forces of salbutamol sulfate, budesonide, and formoterol fumarate dihydrate were investigated by *in situ* atomic force microscopy (AFM) in a model propellant 2H,3H perfluoropentane. The surface thermodynamic properties were determined by contact angle (CA) and inverse gas chromatography (IGC). Experimental data were compared with theoretical work of adhesion/cohesion using a surface component approach (SCA), taking into account both dispersive and polar contributions of the surface free energy.
Results. Results indicated that the measured forces of interaction between particles in model propellant could not be accounted for by theoretical treatment of the dispersive surface free energies via CA and IGC. A correlation between theoretical work of adhesion/cohesion and AFM measurements was observed upon the introduction of the polar interfacial interactions within the SCA model.
Conclusions. It is suggested that the polar contributions of the surface free energy measurements of particles may play a crucial role in particle interaction within propellant-based systems. Together with the application of a SCA model, this approach may be capable of predicting suspension stability of pMDI formulations.

KEY WORDS: AFM; pMDI; surface energy; suspension.

INTRODUCTION

The delivery of drug particulates to the respiratory tract has become an essential and effective means of treating a variety of pulmonary disorders, including asthma, chronic obstructive pulmonary disease, bronchitis, and cystic fibrosis (1,2). Such popularity can be related to the relative small dose required for effective and often rapid onset of the therapeutic effect while reducing systemic exposure and minimizing drug-related side effects. The pressurized metered dose inhaler (pMDI) remains the most commonly prescribed device for therapeutic aerosol delivery (3). Currently, this dosage form may contain hydrofluoroalkane (HFA) propellants alongside the drug substance, surfactant, and cosolvents. The formulation of a pMDI can generally be subdivided into two categories: solution- and suspension-based systems. Suspension-based pMDIs are generally the most popular because drugs are generally insoluble in the propellant system and thus solubilization in a nonpolar solvent and/or the potential for chemical degradation are obviated (4).

Non-aqueous suspensions raise particular formulation challenges. Their preparation requires careful consideration of the interaction between drug particulates in liquefied propellant, and various components of the pMDI device (3,4). Previous approaches have investigated the behavior of pMDI system mainly through empirical measurements of the flocculation behavior of particulates, and analytical measurement of the loss of drug within the device (4,5). Techniques such as zetametry, sedimentation, and particle size analysis (6), microscopy and spectroscopy (7,8) are routinely used to measure pMDI formulation stability. However, indirect and direct measurement of the various interactions, which govern their behavior, have seldom been performed. The use of surface energetic measurements, via contact angle (CA) and inverse gas chromatography (IGC) measurements, together with the use of particle interactions theories have enabled indirect evaluation of the particulate interactions (9–12). Moreover, the advent of the atomic force microscope colloid probe approach (13) provides an approach to directly quantify interactions between drug particles and formulation components in model pMDI systems (14,15).

The primary aim of the study was to correlate atomic force microscopy (AFM) measurements of interparticulate forces with theoretical measurements of the interfacial free energy of particle interactions via surface free energy data and to gain a greater understanding of the thermodynamic and surface physicochemical properties that directly influence particle-particle interactions in suspension-based pMDI systems. The quantitative study of adhesion/cohesion interac-

[1] Pharmaceutical Technology Research Group, Department of Pharmacy, University of Bath, Bath, United Kingdom.
[2] AstraZeneca R&D Charnwood, Loughborough, United Kingdom.
[3] To whom correspondence should be addressed. (e-mail: r.price@bath.ac.uk)

tions in a model pMDI was carried out by *in situ* colloid probe AFM. The surface thermodynamic properties of the active ingredients were measured using contact angle (CA) and inverse gas chromatography (IGC). The relationship between AFM measurements and the interfacial behavior of the colloid particles was modeled using a surface component approach (SCA) derived from Fowkes, Good-Girifalco, and van Oss models (9,16,17).

Particle Interaction Theory

Interactions between colloidal particles are usually described by the Derjaguin-Landau-Verwey-Overbeek (DLVO) theory (18,19). The DLVO theory considers two types of interactions: a dispersive attractive interaction of the Lifshitz van der Waals (LW) type and a predominately repulsive electrostatic interaction due to the interpenetration of electrical double layers. The application of the DLVO theory for the stabilization of drug suspensions in non-aqueous pMDI media has not been fully validated (20). The possible limitation of the approach, which has been successfully used to describe the behavior of aqueous suspensions, is the absence of an ionic double layer (21,22). A quick theoretical calculation of the repulsive electrostatic energy of interaction between 1-μm solid particles as a function of interparticulate distances in liquefied propellants with varying dielectric constants (reciprocal thickness of the diffuse double layer set at 2×10^6 cm^{-1}) show that the electrostatic repulsive forces acting between particles are small. This may be attributed to the overlap of very diffusive electrical double layers due to a combination of low dielectric constants and low ionic strengths (23). Thus, the attractive LW forces are thought to predominate at all separation distances. As a result, theoretical descriptions of non-aqueous drug suspensions via a DLVO approach are very limited, as they fail to adequately predict the stability of these formulations (4,20).

An alternative approach to the DLVO theory has been proposed by van Oss (9,24,25). The approach decomposes the surface energetics (i.e., surface tension or contact angle values) into independent contributions and in particular introduces a polar acid-base (AB) (electron donor/electron acceptor) component (9). The corresponding polar free energy of interaction (AB), which can be repulsive or attractive (depending on the chemical structure, suspending medium properties and surface potential) can control the total energy of interaction at small separation distances. According to this surface contribution approach (SCA), the total surface free energy of a solid is determined by the LW dispersive component (γ^{LW}) and the polar AB component (γ^{AB}) as given in Eq. (1):

$$\gamma^{TOT} = \gamma^{LW} + \gamma^{AB} \tag{1}$$

The total free energy of interaction between two surfaces in a liquid medium is subsequently defined as the sum of LW dispersive interactions, the polar component (AB), and electrostatic double layer (EL) interactions [Eq. (2)]:

$$\Delta G^{TOT} = \{\Delta G^{LW} + \Delta G^{AB}\} + \Delta G^{EL} \tag{2}$$

In the absence of an electrostatic influence, the interaction energy between solid surfaces (S) immersed in a liquid (L) can be expressed by the interfacial free energy (ΔG_{SLS}), see Eq. (3). This in turn can be related to the solid-liquid interfacial tension via:

$$\Delta G_{SLS} = \Delta G^{LW} + \Delta G^{AB} = -2\gamma_{SLS} = -2(\gamma_{SLS}^{LW} + \gamma_{SLS}^{AB}) \tag{3}$$

The interfacial energy parameters for the LW and AB contributions between similar solids (1) in a liquid (3) can be obtained from the surface free energy and surface tensions of the solid and liquid by using the Good-Girifalco-Fowkes approach (16,17) [Eq. (4)]:

$$\Delta G_{131} = -2\left[\left(\sqrt{\gamma_1^{LW}} - \sqrt{\gamma_3^{LW}}\right)^2 + 2\left(\sqrt{\gamma_1^+\gamma_1^-} + \sqrt{\gamma_3^+\gamma_3^-} - \sqrt{\gamma_1^+\gamma_3^-} - \sqrt{\gamma_1^-\gamma_3^+}\right)\right] \tag{4}$$

For liquids with very low polarity ($\gamma_3^+ = \gamma_3^- \sim 0$ mJ/m^{-2}), the free energy of interaction can be simplified to [Eq. (5)]:

$$\Delta G_{131} = -2\left(\sqrt{\gamma_1^{LW}} - \sqrt{\gamma_3^{LW}}\right)^2 - 4\sqrt{\gamma_1^+\gamma_1^-} \tag{5}$$

Hence, knowledge of the surface energy of the solid (γ_1^{LW}, γ_1^+, and γ_1^-) and the surface tension of the liquid (γ_3^{LW}, γ_3^+ and γ_3^-) enables the determination of interaction energy between particles within the media.

Similarly, the energy of interaction between dissimilar solid surfaces (1 and 2) in a liquid (3) can be calculated using the following expression (6):

$$\Delta G_{132} = 2\left[\sqrt{\gamma_1^{LW}\gamma_3^{LW}} + \sqrt{\gamma_2^{LW}\gamma_3^{LW}} - \sqrt{\gamma_1^{LW}\gamma_2^{LW}} - \gamma_3^{LW} + \sqrt{\gamma_3^+}\left(\sqrt{\gamma_1^-} + \sqrt{\gamma_2^-} - \sqrt{\gamma_3^-}\right) + \sqrt{\gamma_3^-}\left(\sqrt{\gamma_1^+} + \sqrt{\gamma_2^+} - \sqrt{\gamma_3^+}\right) - \sqrt{\gamma_1^+\gamma_2^-} - \sqrt{\gamma_1^+\gamma_2^+}\right] \tag{6}$$

In an apolar medium (γ_3^+ and $\gamma_3^- \sim 0$ mJ m^{-2}), the energy of interaction can be used in the simplified form (7):

$$\Delta G_{132} = 2\left[\sqrt{\gamma_1^{LW}\gamma_3^{LW}} + \sqrt{\gamma_2^{LW}\gamma_3^{LW}} - \sqrt{\gamma_1^{LW}\gamma_2^{LW}} - \gamma_3^{LW} - \sqrt{\gamma_1^+\gamma_2^-} - \sqrt{\gamma_1^+\gamma_2^+}\right] \tag{7}$$

The influence of the van der Waals interactions on the force of adhesion can be related to the thermodynamic work of adhesion ($W_{ad} = -\Delta G_{SLS} = -\Delta G_{132}$) through the Hertz approximation for elastic bodies (26), which takes into account the separation distance and the contact geometry of interacting surfaces. Two models can be used for this purpose, the Johnson, Kendall, and Roberts (JKR) and the Derjaguin, Müller, and Toporov (DMT) models (27,28). Their validity have been found to depend on the interacting materials and their geometries. The DMT theory is typically valid for small particles, low surface energies and high elastic moduli, whilst the converse is true for the JKR model.

The general form of the relationship of the force of adhesion with the energy (derived for LW interactions between two spherical particles) can be expressed as in Eq. (8) (27):

$$F_{ad} = n\pi R^* W_{ad} \tag{8}$$

where R^* is the harmonic mean of the particle radii (also called contact radius) and n is a predetermined constant depending on the selected model (n = 3/2 for JKR and n = 2 for the DMT model).

MATERIALS AND METHODS

Materials

Micronized salbutamol sulfate, budesonide, and formoterol fumarate dihydrate were supplied by AstraZeneca (Loughborough, Leicestershire, UK) and were used as received. The model propellant HPFP (2H, 3H perfluoropentane) was supplied by Apollo Scientific (Stockport, Derbyshire, UK). The purity of HPFP was in excess of 99.9%, with a moisture content less than 9 ppm. Further purification of the HPFP was achieved by filtering and purifying with chromatographic grade acidic and basic alumina (Fluka, Gillingham, UK). This treatment was necessary to remove impurities in the organic liquid that may otherwise directly influence particle adhesion measurements. All organic solvents (diiodomethane and ethylene glycol) used in the study were supplied by BDH (Poole, Dorset, UK) and were of analytical grade. Purified water was prepared by reverse osmosis (MilliQ, Molsheim, France).

Scanning Electron Microscopy

Scanning electron microscopy (SEM) was used to characterize the morphology of the micronized drugs. Powder samples were deposited on adhesive carbon black tabs, which were premounted on aluminum stubs. Particles were coated with a thin gold film using a sputter coater (model S150B, Edwards High Vacuum, Sussex, UK). Samples were imaged using a JEOL 6310 SEM (Jeol, Tokyo, Japan) at 10KeV.

Particle Sizing

Particle sizing of the micronized drug samples were performed using a Mastersizer X (Malvern Instruments Ltd, Malvern, UK). The instrument was equipped with a small volume cell (with a capacity of approximately 20 ml) and a 100 mm lens, allowing particle detection in the size range of 0.5–120 μm. Approximately 1 mg of drug material was suspended in a 0.1% w/v lecithin/cyclohexane solution and sonicated for 10 min at 25°C prior to analysis. The particle size distribution was characterized by the 10th, 50th, and 90th percentile of the cumulative particle undersize frequency distribution. All samples were run as triplicates.

Preparation and Characterization of Drug Crystals

One of the limitations of the colloidal probe AFM approach to date has been associated with dramatic inter- and intra-variations in cohesion and adhesion measurements related to slight differences in contact geometry between interacting surfaces. In this study, direct comparisons of the force of interaction between specific colloid probes and an array of substrate materials was made possible by crystallizing molecularly smooth crystals from solution. Single crystals of salbutamol, budesonide, and formoterol were heterogeneously nucleated and grown on a borosilicate glass substrate using a sitting drop technique, described elsewhere (29). This process produced planar crystals with large areas of sub-nanometre smooth surfaces.

AFM Topographical Measurements

The surface topography of the drug crystal surfaces was investigated using the AFM in its conventional imaging mode. Imaging was conducted in Tapping Mode operation with a high-aspect-ratio silicon probe (OTESP, Digital Instruments, UK), at a scan rate of 0.7 Hz. All AFM studies were performed using a commercially available Multi Mode AFM with a Nanoscope III controller [Digital Instruments (DI), Cambridge, UK]. The root mean squared surface roughness (R_{rms}) of the deviations from the average height was calculated from the AFM height data over a 5 μm × 5 μm area via:

$$R_{rms} = \sqrt{\frac{1}{n}\sum_{i=1}^{n} y_i^2} \tag{9}$$

where n is the number of points in topography profile and y_i is the heights of the surface asperities (i).

Model Drugs Compact Preparation

Contact angle measurements were obtained using the sessile drop method on model compacts of the micronized drug. Compacts were prepared by direct compression using a servo hydraulic press (model 25010, Specac Ltd., Kent, UK). Approximately 250 mg of the micronized material was weighed into a 10-mm stainless steel die, spread evenly in the die, and compacted with a compression force of 10 kN. Compacts were stored in sealed containers in a controlled environment (25°C, 44% RH) for at least 24 h prior to use.

AFM Colloid Probe Measurements

Colloid probes were prepared by mounting an individual micronized drug particle (approximate diameter 5 μm) onto a V-shaped tipless cantilever (spring constant k = 0.32 N/m, DNP-020, DI, Cambridge, UK) using a quick-setting epoxy resin (30). Extreme care was taken during drug probe preparation to limit the amount of drug-glue contact. The micromanipulation technique is described in detail elsewhere (31). The measurement of the forces of adhesion and cohesion between individual particles and their respective crystal surfaces were carried out in HPFP with an *in situ* liquid AFM cell (7,8). It is important to note that conventional AFM systems are currently limited to studies in air and/or low vapor pressure liquid environments. Thus, HPFP was chosen for its similarities to the physicochemical properties of HFA227, used in pMDIs (32). The use of HPFP as a model system for studying the behavior of pMDIs, when characterization methods cannot be adapted to the pressure regime, has been extensively studied by Rogueda (32).

Force-distance profiles were recorded by measuring the deflection of the cantilever as the substrate surface was ramped into and out of contact with the cantilever in a stepwise fashion (30,33,34). By applying Hooke's law, $F = kx$ (where x is the deflection of the cantilever and k the spring constant), a quantitative measurement of the force of adhesion can be obtained. Multiple force distance curves (n = 512) were determined between each drug probe and crystal surface over a 5 μm × 5 μm area with the following settings: approach-retraction cycle 0.5 μm, cycle rate 4.07 Hz, and a loading force of 20 nN. Each study was performed with three probes of each drug. To avoid significant variations in contact

area between an individual probe and the respective substrate surfaces, a great deal of care and attention were taken to maintain the integrity of the colloid probe throughout the study.

To further overcome the limitation of not knowing the true area of contact between drug probes, the cohesive and adhesive forces ratios were analyzed and compared using the recently developed cohesive-adhesive balance (CAB) analysis procedure (35). This approach provides a quantitative measurement of the adhesive and cohesive balance of the interactive forces within a formulation. The CAB analysis procedure allows AFM measurements of inter-particulate forces to be directly correlated to the thermodynamic work of cohesion and adhesion of interacting surfaces via surface energy measurements. For a particulate interacting with two surfaces (one alike and one different) the cohesive-adhesive balance between the two materials can be expressed by:

$$\frac{F_{coh}}{F_{adh}} = \frac{R^*_{cohesion}\, n\pi W_{coh}}{R^*_{adhesion}\, n\pi W_{adh}} \tag{10}$$

where F_{coh} and F_{adh} are the cohesive and adhesive forces measured by AFM, and W_{coh} and W_{adh} are the thermodynamic work of cohesion and adhesion, respectively. Assuming the contact mechanics of the cohesive and adhesive interaction follow the same theoretical model, the ratio of the van der Waals forces for a series of colloidal probes should be constant and directly proportional to the thermodynamic ratio of the work of cohesion and adhesion of the interfacial interactions calculated via the surface free energy measurements of the interacting particles. Furthermore, determining the balance of van der Waals forces for a series of colloidal probes via AFM measurements overcomes the need to determine variations in the spring constant (k) of each individual AFM cantilever.

Contact Angle Measurements

The contact angle of the powder compact surfaces were measured using the sessile drop method (10,16,36–38) with a NRL goniometer (Ramé-Hart, Inc., Mountain Lakes, NJ, USA) equipped with a 2.3× objective lens, and a 10× Ramsden type eyepiece. A liquid drop was introduced onto the substrate surface via a microsyringe. Advancing contact angles were measured for three different liquids (water, diiodomethane, and ethylene glycol) at room temperature (20°C). A summary of the surface tension components of the liquids used in the direct contact angle determination (9) are presented in Table I. The surface energy parameters of the compact surfaces were determined using the Young-Duprè equation, which requires the contact angle (θ) measurements for a minimum of three liquids (one apolar and two polar) via the following relationship:

$$\gamma_L(1+\cos\theta) = 2\left(\sqrt{\gamma_S^{LW}\gamma_L^{LW}} + \sqrt{\gamma_S^{+}\gamma_L^{-}} - \sqrt{\gamma_S^{-}\gamma_L^{+}}\right) \tag{11}$$

where γ_S and γ_L are the surface free energies of the solid and the liquid, respectively.

Table I. Surface Tension Components and Parameters of Liquids Used in CA Measurements at 20°C (van Oss, 1994) (14)

	Surface tension components and parameters ($mJ \cdot m^{-2}$)			
	γ^{LW}	γ^{+}	γ^{-}	γ^{AB}
Diiodomethane	50.8	~0	0	0
Water	21.8	25.5	25.5	51.0
Ethylene glycol	29.0	1.92	47.0	19.0

Inverse Gas Chromatography

Inverse gas chromatography (IGC) provides a means of determining both the dispersive and polar components of surface free energy for micronized drugs (11,12), without potential modification of the surface properties of the particles upon compaction (39). The surface free energy characteristics of the micronized powders were determined using a commercially available IGC (IGC 2000, Surface Measurement Systems Ltd, London, UK). The dispersive component of the solid surface free energy (γ_s^d) can be calculated by measuring the retention time (volume) of a series of alkanes of known γ_l^d injected at an infinite dilution using the following relationship (40):

$$RT \ln V_N = 2N\sqrt{\gamma_s^d}\, a\sqrt{\gamma_l^d} + C \tag{12}$$

where R is the gas constant, T the temperature, N is Avogadro's number, a is the projected surface area of the sample probe, γ_l^d the dispersive component of the probe, and V_N the net volume of carrier gas required to elute the probe molecules from the column (corrected for column dead time and compression factors). This procedure is based on the determination of a linear relationship between the retention volume ($RT\ln V_N$) of the nonpolar probe against $a(\gamma_l^d)^{0.5}$. The dispersive component of the surface free energy of the solid can be calculated from the slope.

The electron donor and electron acceptor properties of the micronized powders were determined by IGC using polar liquids in the vapor phase. The specific (polar) interactions ΔG_{sp} can be related to the acidic or electron accepting parameter (K_a) and the basic or electron donor parameter (K_b) by the following equation:

$$\frac{\Delta G_{sp}}{AN^*} = \left(\frac{DN}{AN^*}\right)K_a + K_b \tag{13}$$

where DN is an electron donor or base number characterized according to Gutmann (41) and AN^* is an electron acceptor or acid number (42). The values of K_a and K_b of the powder samples were determined from the gradient and the intercept of the line obtained plotting $\Delta G_{sp}/AN^*$ vs. DN/AN^*.

Approximately 1.0 g of the micronized powder was weighed into standard glass IGC columns and plugged with glass wool. Each column was tapped for 5 min, using the minimum setting on a jolting voltameter (Surface Measurement Systems Ltd, London, UK) to a produce "homogeneous" powder bed. Each column was purged in the IGC at 0% RH, at 318.05 K with dry nitrogen for 3 h prior to analysis to remove surface moisture. The retention time of a series of *n*-alkanes (hexane to decane) and polar (ethanol, chloroform, dioxane, ethyl acetate, and acetone) probes were detected at infinite dilution with a flame emission detector. Column settings and run times for all three drugs were optimized at 318.05 K. Each column was analyzed twice.

Statistical Analysis

The statistical analysis of forces of interaction between individual colloid probes and respective substrates were compared using one-way ANOVA. The results were found to be significantly different based upon 95% probability values ($p < 0.05$).

RESULTS AND DISCUSSION

Physical Characterization

The morphology and size of the micronized drugs were fully characterized by SEM and laser light diffraction.

Scanning Electron Microscopy

Representative scanning electron micrographs of the micronized drugs are shown in Fig. 1. In general, all three drugs exhibited irregular crystal morphology with clear variations in crystal size, which correlated well with particle size measurements.

Particle Size

Micronized budesonide was found to have a median equivalent volume diameter of 3.24 μm, with over 82% of particles below 5 μm. By comparison, formoterol was found to have a median equivalent volume diameter of 2.69 μm, with 93% of particles below 5 μm. Salbutamol was found to have the largest median equivalent volume diameter of 6.61 μm, with 46% of particles below 5 μm. In general, the particle sizing data agreed well with SEM observations, with drug samples falling within the required size range for pulmonary delivery.

Determination of Contact Angle and Relative Surface Energy Values for Powder Compacts

The surface energy components obtained by CA (9,10) and IGC measurements are presented in Table II. Both CA and IGC values follow a similar trend. The highest dispersive (LW) values were measured for budesonide by both techniques, followed by formoterol and then salbutamol. These observations are in general agreement with related studies of the ranking of the dispersive parameters of pharmaceutical powders (43,44). A direct comparison of the data between the two techniques is rather difficult due to the variations in the experimental and theoretical approaches (11). The acidic and basic components of the powder samples from IGC measurements are not consistent with the results obtained from CA measurements. A quantitative determination of the polar components from IGC would require specific knowledge of the surface contact area of the polar component of the solvent probes with the solid. This limitation currently precludes the use of the surface component approach in determining the polar free energy of interaction via IGC measurements.

Determination of the Theoretical Work of Adhesion/ Cohesion

The dispersive and polar components of the work of cohesion and adhesion of the drug particles were calculated from the surface energy measurements derived from the CA studies and the surface tension value of HPFP. The dispersive LW work of cohesion and adhesion was obtained using the Good-Girifalco-Fowkes combining rule from the IGC measurements [Eq. (4)]. The thermodynamic work of adhesion and cohesion were calculated for the various particle-particle combinations in HPFP, and are shown in Table III.

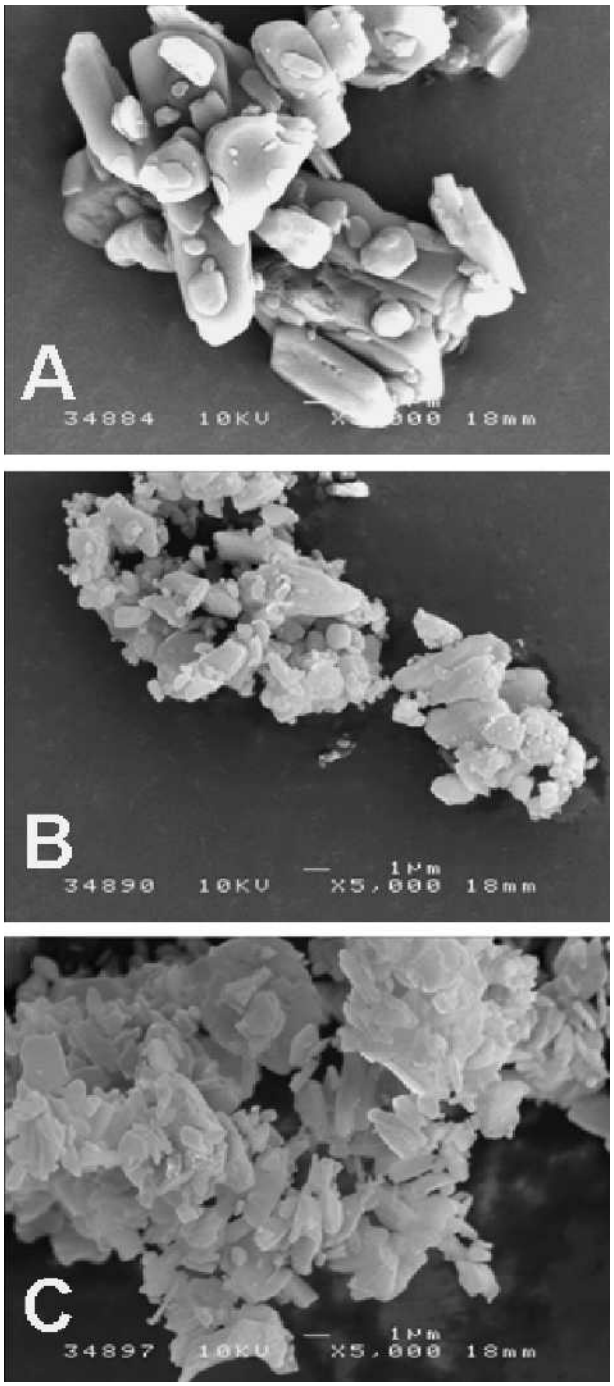

Fig. 1. Scanning electron micrographs of micronized salbutamol sulfate (A), budesonide (B), and formoterol fumarate dihydrate (C).

Comparison of the LW and AB work of cohesion/ adhesion for salbutamol suggests that both the cohesive and adhesive interactions are dominated by polar interactions. The dispersive part of the interactions is greatest for the salbutamol-budesonide combination and smallest for salbuta-

Table II. Surface Free Energy Components Obtained via CA and IGC Measurements

	Surface energy components from CA ($mJ \cdot m^{-2}$)				Surface energy components from IGC ($mJ \cdot m^{-2}$)		
	γ^{LW}	γ^{+}	γ^{-}	γ^{AB}	γ^{LW}	K_a	K_b
Salbutamol sulphate	46.5 ± 0.7	8.3 ± 1.5	18.5 ± 1.2	24.6 ± 2.5	39.1 ± 1.3	0.085 ± 0.002	0.029 ± 0.001
Budesonide	49.1 ± 0.4	0.3 ± 0.4	22.5 ± 3.8	4.6 ± 2.9	62.9 ± 1.7	0.113 ± 0.002	0.013 ± 0.001
Formoterol	48.5 ± 0.4	0.1 ± 0.2	35.0 ± 3.0	3.2 ± 3.0	51.2 ± 0.7	0.93 ± 0.002	0.026 ± 0.001

Values are mean ± SD, n = 3.

mol-salbutamol. This is true for both CA and IGC measurements. The total energy, that is, when both LW and AB components are taken into consideration, is greater for the cohesive salbutamol interactions, followed by the adhesion energies of salbutamol-formoterol and salbutamol-budesonide.

For budesonide, the LW components dominate the AB interactions for cohesive and adhesive (budesonide-formoterol) energies. However, the polar contributions are higher for the budesonide-salbutamol adhesive energy. Interestingly, the total theoretical work of interaction is greater for budesonide-salbutamol, with a strong polar component.

For formoterol, the dispersive energy component is greater for the budesonide-formoterol adhesion. The polar energy component is greater for the formoterol-salbutamol adhesion, and the total energy is greatest for this system. Thus, further highlighting the importance of polar energetic components in particle interactions.

This brief theoretical treatment of particle interactions derived from surface energetic components highlights the possibility of significant variations between interfacial interactions depending on whether they are calculated from dispersive components or a combination of polar and dispersive contributions. The fact that polar components of the solids should be taken into account in non-polar liquids is counter-intuitive and cannot be overlooked.

In an attempt to quantify these theoretical predictions, the thermodynamic work of adhesion and cohesion was compared with adhesive and cohesive force measurements via AFM experiments.

Atomic Force Microscopy Analysis

Measurement of pull-off forces between individual particles and substrate surfaces by AFM and the influence of complex interactive forces on particle adhesion have been reported previously (15,31,45). However, wider application of the AFM technique for preformulation development has been limited by the dramatic influence of the contact area between contiguous surfaces on quantitative force measurements. Although attempts to quantify the contact radii of the asperities of the colloid probes have been made (45), normalization and direct comparison of cohesive and adhesive forces in multicomponent systems remains onerous, due to the limited knowledge of the true contact area between probe and a substrate of varying surface roughness. Furthermore, efforts to predict adhesive interactions using theoretical approaches and surface energy measurements have, to date, proved unsatisfactory (46). Theoretical estimates are often several orders of magnitude greater than experimental measurements (47,48). The most plausible explanation for this discrepancy is the variation in the mesoscopic contact area between contiguous surfaces from the expected macroscopic dimensions. These difficulties can, however, be overcome by the use of the novel cohesive-adhesive balance (CAB) analysis procedure developed by Begat *et al.* (35).

Table III. Theoretical Values of the Thermodynamic Work of Adhesion and Cohesion for Particulate Interactions in HPFP, Calculated via Equation VII

	W^{LW} IGC	W^{LW} CA	W^{AB} CA	W^{TOT} CA
		Cohesive energies		
Salbutamol-Salbutamol	13.15	19.62	49.40	69.00
Formoterol-Formoterol	24.08	21.50	7.74	29.24
Budesonide-Budesonide	36.04	22.04	11.12	33.14
		Adhesive energies		
Salbutamol-Formoterol	17.79	20.54	36.82	57.34
Salbutamol-Budesonide	21.77	20.80	32.26	53.06
Budesonide-Formoterol	29.46	21.76	10.04	31.8

All values are in $mJ \cdot m^{-2}$.

Analysis of Substrates Surfaces

Prior to adhesion studies, the surface roughness on the dominant crystal face of each drug substrate was investigated. Roughness analysis (n = 25, 5 × 5 μm area) of the surface topography for each drug crystal indicated R_{RMS} values of:

Salbutamol, 1.33 nm (±0.04)
Budesonide, 0.68 nm (±0.01)
Formoterol, 1.52 nm (±0.01)

The data suggested extremely smooth surface morphologies, with surfaces exhibiting a root-mean-squared roughness well below 2 nm over a 25 μm^2 area. Although different degrees of roughness did exist between drugs (most likely related to differing crystal growth processes and kinetics during crystallization), the uniform and smooth topography made them highly suitable for maintaining reproducible contact geometry between an individual colloid probe and the substrate surfaces under investigation.

Measurement of Forces of Cohesion and Adhesion

The *in situ* AFM probe technique allowed direct measurements of the cohesion and adhesion between single drug particulates and the dominant crystal faces of each drug material. The integrity of all drug probes was investigated prior to and post measurement using a high-magnification 500× long-working distance optical microscope. In all cases, the drug probes appeared proud of the cantilever surface, with no visible differences between the start and end of the experimental procedure (indicating no macro/microscopic change in drug-probe morphology). The number distribution of each

data set indicated a normal distribution with low variability, suggesting the interaction with a highly smooth substrate surfaces providing a uniform contact geometry for the interacting probe. The specific mean values and standard deviations for the interaction for each drug probe and substrate are provided in Table IV. As expected, comparisons between probes of the same drug (probes 1–3) indicate large variations in adhesion force. This may be explained by the difference in particle size and variations in contact geometry due to the irregular shape of the probes. Without prior knowledge of the true contact area of each probe, inter-probe variations cannot be quantified. However, trends can be discerned for each drug probe and their forces of interactions measured ranked.

Hence, the cohesive salbutamol-salbutamol force of interaction was shown to be stronger than the adhesion salbutamol-formoterol, which in turn was higher than salbutamol-budesonide interactions. The AFM data suggested that the salbutamol-formoterol interaction was approximately twice that of the salbutamol-budesonide adhesion.

For the budesonide probes, the order was budesonide-salbutamol, budesonide-budesonide and budesonide-formoterol. The quantitative AFM data suggested that the adhesive (budesonide-salbutamol) interaction was nine times greater than the cohesive one.

Finally, for formoterol, the rank order was formoterol-salbutamol, formoterol-formoterol, and formoterol-budesonide. AFM data suggested that the formoterol-salbutamol interaction was approximately five times greater than the force of cohesion.

Comparisons Between Thermodynamic Work of Adhesion and AFM Measurements

As previously discussed, the thermodynamic work of adhesion is directly proportional to the force of adhesion. To highlight this relationship and the specific role of the dispersive (LW) and total (LW + AB) interactions, representative plots of the theoretical work of adhesion of the LW (W_{ad}^{LW}) interactions and the influence of acid-base interactions ($W_{ad}^{Tot} = W_{ad}^{LW} + W_{ad}^{AB}$) vs. the force measurements are shown in Fig. 2 (for the case of salbutamol drug probe). It is anticipated that the work of adhesion/cohesion should increase with an increasing force of adhesion/cohesion.

The plots suggest no direct relationship between the separation force measurements and the dispersive component of the work of adhesion (W_{ad}^{LW}) calculated from either IGC or CA measurements (Fig. 2, IGC and CA). However, a positive relationship was observed between the force measurements and the total work of adhesion (W_{ad}^{Tot}) when taking into accounts both the non-polar and polar contributions.

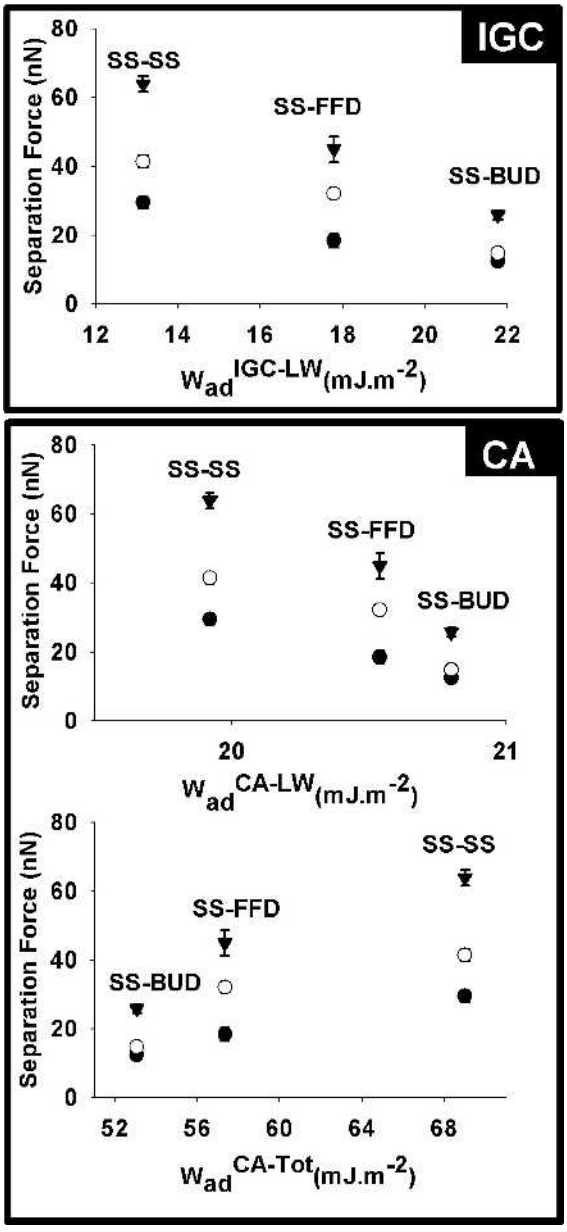

Fig. 2. Plot of the theoretical thermodynamic work of adhesion *vs.* AFM force measurements for salbutamol sulfate drug probes (n = 3 probes, ● = 1; ○ = 2; ▼ = 3). Energies were calculated from IGC and CA measurements. The upper two plots take into account the dispersive contribution only. The lower plot includes the polar as well as dispersive contributions. Key to the abbreviations: salbutamol (SS), formoterol (FFD), and budesonide (BUD).

Table IV. AFM Separation Force Measurements for Micronised Salbutamol Sulphate, Budesonide and Formoterol Fumarate Dihydrate

	Probe								
	Salbutamol			Budesonide			Formoterol		
Substrate	Tip 1	Tip 2	Tip 3	Tip 1	Tip 2	Tip 3	Tip 1	Tip 2	Tip 3
Salbutamol	29.5 ± 1.5	41.5 ± 1.7	63.9 ± 2.3	10.9 ± 1.1	48.2 ± 2.9	71.9 ± 2.2	58.2 ± 2.1	15.3 ± 1.9	11.2 ± 2.4
Budesonide	12.5 ± 0.9	14.8 ± 1.0	25.8 ± 1.3	0.9 ± 0.2	5.0 ± 2.2	7.9 ± 4.0	13.7 ± 0.3	6.7 ± 1.9	3.7 ± 0.2
Formoterol	18.4 ± 1.9	32.1 ± 0.8	45.0 ± 3.7	1.2 ± 1.1	3.7 ± 0.7	6.7 ± 1.4	13.1 ± 0.7	6.2 ± 0.9	4.1 ± 1.3

Values are ± SD, n = 3 probes. All forces are in nN.

Similarly, analysis of the budesonide and formoterol interactions indicated no correlation between the LW work of adhesion (from IGC and CA) and AFM measurements, while the total theoretical work correlated well with experimental AFM data. Such observations suggest that polar interactions between contiguous surfaces play a significant role in particle adhesion/cohesion in non-aqueous media and should not be neglected in predictive theoretical approaches.

Relationship Between CAB Plots and Theoretical Cohesion/Adhesion Ratios

An estimation of the separation force from theoretical treatment of the interfacial interactions via surface energy measurements would require knowledge of the effective contact area of each probe, as indicated by Eq. (8). This limitation precludes direct correlation of individual AFM force measurements for each probe with theoretical measurements of the work of adhesion/cohesion. However, the determination of the force balance for a series of colloid probes using the CAB analysis procedure does allow quantification of the relationship between the theoretical work of cohesion and adhesion and corresponding AFM measurements.

From theory, the cohesion between material 1 and adhesion between material 1 and 2 in a liquid media (3) can be expressed as:

$$\frac{F_{131}}{F_{132}} = \frac{n\pi R^*_{131} W_{131}}{n\pi R^*_{132} W_{132}} \tag{14}$$

where F_{131} and F_{132} are the cohesive and adhesive forces, respectively. Assuming that the tailoring of the substrate surfaces enables equivalence of the contact radii R^*_{131} and R^*_{132}, the relationship between theory and experimental measurements can be discerned. From Eq. (14), the slope of a plot of the force of cohesion *vs.* the force of adhesion for a series of probes would yield the ratio of the thermodynamic work of cohesion to the work of adhesion.

The AFM data and the theoretical estimation of the cohesive-adhesive balance from the thermodynamic surface free energy measurements for salbutamol, budesonide, and formoterol probes are shown in Figs. 3, 4, and 5, respectively. The bisecting (dotted) line in each figure corresponds to the balance between of cohesion and adhesion ($F_{coh} = F_{adh}$, or $W_{adh} = W_{coh}$). The relative position of the AFM data points with respect to the bisector is a direct indication of the cohesive and adhesive tendencies of the drug particles considered. Data below the bisector indicate an affinity for the probe material to develop adhesive interactions ($F_{adh} > F_{coh}$). Conversely, data above the bisector denote dominant cohesive properties.

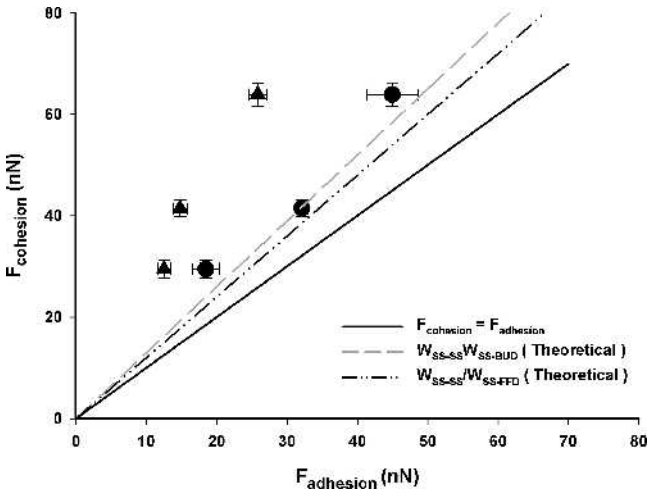

Fig. 3. Relationship between AFM cohesion and adhesion measurements for salbutamol sulfate probes (SS, n = 3) illustrated as a CAB plot. The bisecting (solid) line is the equilibration of the cohesion and adhesion. Dotted lines are theoretical ratios calculated from surface component approach with polar and dispersive contributions. ▲, budesonide (BUD) substrate; ●, formoterol (FFD) substrate.

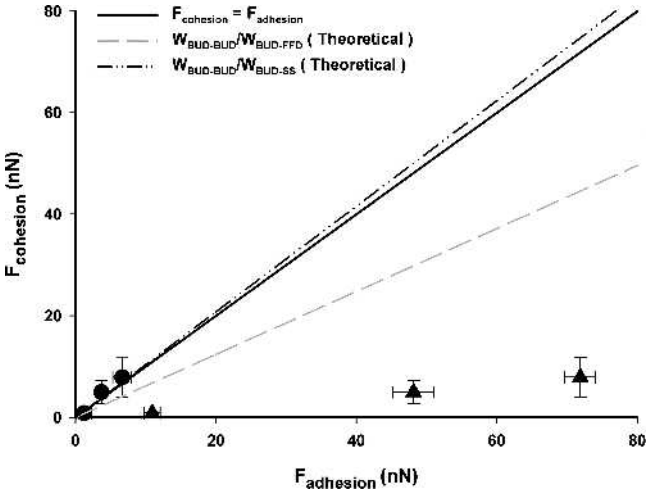

Fig. 4. Relationship between AFM cohesion and adhesion measurements for budesonide probes (BUD, n = 3) illustrated as a CAB plot. The bisecting (solid) line is the equilibration of the cohesion and adhesion. Dotted lines are theoretical ratios calculated from surface component approach with polar and dispersive contributions of the surface free energy measurements. ▲, formoterol (FFD) substrate; ●, salbutamol (SS) substrate.

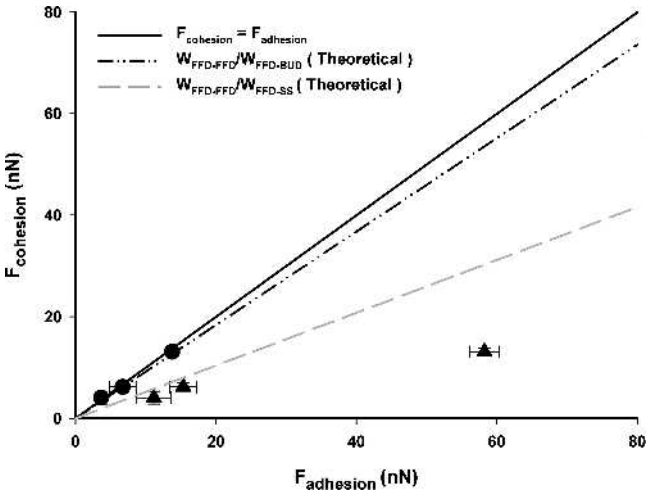

Fig. 5 Relationship between AFM cohesion and adhesion measurements for formoterol fumarate dihydrate probes (FFD, n = 3) illustrated as a CAB plot. The bisecting (solid) line is the equilibration of the cohesion and adhesion. Dotted lines are theoretical ratios calculated from surface component approach with polar and dispersive contributions. ▲ = salbutamol (SS) substrate; ● = budesonide (BUD) substrate.

Table V. Linear Regression Analysis and Measurements of Cohesive/Adhesive Ratios via AFM Measurements Together With the Theoretical Ratios of the Cohesive/Adhesive Interactions

	Experimental ratio $F_{cohesion}/F_{adhesion}$	R^2 $F_{cohesion}/F_{adhesion}$	Theoretical ratio $W_{cohesion}/W_{adhesion}$
Salbutamol-Budesonide	2.41	0.9880	1.30
Salbutamol-Formoterol	1.29	0.9875	1.20
Budesonide-Salbutamol	0.11	0.9958	0.62
Budesonide-Formoterol	1.24	0.9832	1.04
Formoterol-Salbutamol	0.21	0.9005	0.52
Formoterol-Budesonide	0.94	0.9960	0.92

Analysis of Fig. 3 suggested salbutamol to be more cohesive than adhesive, when interacting with formoterol and budesonide. This is in accordance with the theoretical predictions of the total work of adhesion/cohesion shown in Table III.

Similar analysis of CAB data for the budesonide drug probes (Fig. 4) suggested that budesonide was more adhesive with salbutamol than cohesive with itself. The theoretical approach was in agreement with this tendency for an adhesive interaction. Similar agreement between theory and experiment was found for the budesonide-formoterol interactions.

The CAB and theoretical analysis of formoterol interactions (Fig. 5) suggested that formoterol was biased toward adhesion. This again confirmed the experimental and theoretical findings.

A linear regression analysis of the balance of the cohesive and adhesive forces as measured by AFM was performed to calculate the cohesive/adhesive force ratio. These ratios are summarized in Table V, together with the theoretical ratio of the work of cohesion to the work of adhesion. There is a good correlation between the experimental and theoretical ratios, although absolute values are not well correlated, albeit of the same order of magnitude. The two approaches suggest the same bias toward either adhesive or cohesive interactions. The discrepancy between experimental and theoretical measurements, which is of greatest significance for interactions involving salbutamol, may relate to a slight polarity of the model liquid propellant that has not been taken into account. This for instance is known to affect liquid-liquid surface tension predictions. Other possible reasons could be related to the AFM measurements being conducted on the dominant face of each drug crystal, while the surface energy values were calculated from contact angles measurements derived from compacts of micronized drug. Thus, it is reasonable to assume that the less dominant faces may influence the measurements. The relationship between face specific surface free energy and work of adhesion is a subject of ongoing investigations.

The theoretical model developed in this work and its correlation with direct AFM force measurement may provide the basis for a powerful pMDI preformulation tool. This understanding of the influence of the physicochemical properties of colloid particles on particulate interactions may provide the formulation scientist with a guide to improving the stability of pMDI suspensions and the behavior of the system under development.

CONCLUSIONS

Direct measurements of the interaction forces (via AFM measurements) responsible for the stability of colloid particles in pMDI formulations indicate a fine balance between adhesive and cohesive tendencies. A relationship between the theoretical interfacial thermodynamics, derived from the surface component approach, and experimental force measurements were demonstrated. Correlation of the experimental measurements with theory required the introduction of the polar as well as dispersive components of surface energies of the interacting solids. This combined approach may provide a novel means of predicting suspension stability of pMDI formulations.

REFERENCES

1. D. Ganderton and T. Jones. *Drug Delivery to the Respiratory Tract*, Academic Press, London, 1987.
2. J. S. Patton. Mechanisms of macromolecule absorption by the lungs. *Adv. Drug Deliv. Rev.* **19**:3–36 (1996).
3. D. L. Ross and B. J. Gabrio. Advances in metered dose inhaler technology with the development of a chlorofluorocarbon free drug delivery system. *J. Aerosol Med.* **12**:151–160 (1999).
4. H. D. C. Smyth. The influence of formulation variables on the performances of alternative propellant-driven metered dose inhalers. *Adv. Drug Deliv. Rev.* **55**:807–828 (2003).
5. D. Ganderton. Patients, devices and formulations. *J. Aerosol Med.* **23**:441–444 (2003).
6. J. A. Ranucci, S. Dixit, R. N. J. Bray, and D. Goldman. Controlled flocculation in meterd-dose aerosol suspensions. *Pharmacetical Technology* **0**:68–73 (1990).
7. Y. Michael, M. J. Snowden, B. Z. Chowdhry, I. C. Ashurst, C. J. Davies-Cutting, and T. Ripley. Characterisation of the aggregation behaviour in a salmeterol and fluticasone propionate inhalation aerosol system. *Int. J. Pharm.* **221**:165–174 (2001).
8. E. M. Phillips, P. R. Byron, and R. N. Dalby. Axial-ratio measurements for early detection of crystal-growth in suspension-type metered dose inhalers. *Pharm. Res.* **10**:454–456 (1993).
9. C. J. van Oss. *Interfacial Forces in Aqueous Media*, Marcel Dekker, New York, 1994.
10. R. J. Good. Contact-angle, wetting, and adhesion—a critical-review. *J. Adhes. Sci. Technol.* **6**:1269–1302 (1992).
11. M. D. Ticehurst, R. C. Rowe, and P. York. Determination of the surface properties of two batches of ss by inverse gas chromatography. *Int. J. Pharm.* **111**:241–249 (1994).
12. O. Planinsek and G. Buckton. Inverse gas chromatography: considerations about appropriate use for amorphous and crystalline powders. *J. Pharm. Sci.* **92**:1286–1294 (2003).
13. G. Binnig and C. F. Quate. Atomic force microscope. *Phys. Rev. Lett.* **56**:930–933 (1986).
14. R. Ashayer, P. F. Luckham, S. Manimaaran, and P. Rogueda. Investigation of the molecular interactions in a pMDI formulation by atomic force microscopy. *Eur. J. Pharm. Sci.* **21**:533–543 (2004).
15. P. Young, R. Price, D. Lewis, S. Edge, and D. Traini. Under pressure: predicting pressurized metered dose inhaler interactions using the atomic force microscope. *J. Colloid Interface Sci.* **262**:298–302 (2003).
16. F. M. Fowkes. Additivity of intermolecular forces at interfaces. I. Determination of the contribution to surface and interfacial ten-

sion of dispersion forces in various liquids. *J. Phys. Chem.* **67**: 2538–2541 (1963).
17. R. J. Good and L. A. Girifalco. A theory for estimation of surface and interfacial energies. III. Estimation of surface energies of solids from contact angle data. *J. Phys. Chem.* **64**:561–565 (1960).
18. B. V. Derjaguin and L. D. Landau. Theory of the stability of strongly charged lyophobic sols and of the adhesion of strongly charged particles in solutions of electrolytes. *Acta Physicochimica. U.S.S.R.* **14**:663 (1941).
19. E. J. W. Verwey and J. T. G. Overbeek. *Theory of the Stability of Lyophobic Colloids*, Elsevier, Amsterdam, 1948.
20. C. Vervaet and P. R. Byron. Drug surfactant propellant interactions in HFA formulations. *Int. J. Pharm.* **186**:13–30 (1999).
21. R. J. Pugh, T. Matsunaga, and F. M. Fowkes. The dispersability and stability of carbon black in media of low dielectric constant. I: Electrostatic and steric contributions to colloidal stability. *Colloids Surf.* **7**:183–207 (1983).
22. A. Kitahara. Zeta potential in non-aqueous media and its effect on dispersion stability. *Prog. Organic Coatings* **2**:81–98 (1974).
23. D. A. Wyatt and B. Vincent. Electrical effects in non-aqueous systems. *J. Biopharm. Sci.* **3**:27–31 (1989).
24. J. A. Brant and A. E. Childress. Assessing short-range membrane-colloid interactions using surface energetics. *J. Membr. Sci.* **203**:257–273 (2002).
25. J. A. Brant and A. E. Childress. Colloidal adhesion to hydrophilic membrane surfaces. *J. Membr. Sci.* **241**:235–248 (2004).
26. H. Hertz. On the contact of elastic solids. *J. Reine Angew. Math.* **92**:156–171 (1882).
27. K. Johnson, K. L. Kendall, and A. D. Roberts. Surface energy and the contact of elastic solids. *Proc. R. Soc. Lond. A* **324**:301–313 (1971).
28. B. V. Derjaguin, V. M. Müller, and Y. P. Toporov. Effect of contact deformations on the adhesion of particles. *J. Colloid Interface Sci.* **53**:314–326 (1975).
29. G. Rhodes. *Crystallography—Made Crystal Clear*, Academic Press, New York, USA, 1993.
30. W. A. Ducker, T. J. Senden, and R. M. Pashley. Direct measurement of colloidal forces using an atomic force microscope. *Nature* **353**:239–241 (1991).
31. P. M. Young, R. Price, M. J. Tobyn, M. Buttrum, and F. Dey. The influence of relative humidity on the cohesion properties of micronised drugs used in inhalation therapy. *J. Pharm. Sci.* **93**:753–761 (2004).
32. P. G. A. Rogueda. HPFP, a model propellant for pMDIs. *Drug Dev. Ind. Pharm.* **29**:39–49 (2003).
33. H. Mizes, M. Ott, E. Eklund, and D. Hays. Small particle adhesion: measurement and control. *Colloids and Surfaces A* **165**:11–23 (2000).
34. R. Price, P. M. Young, S. Edge, and J. N. Staniforth. The influence of relative humidity on particulate interactions in carrier-based dry powder inhaler formulations. *Int. J. Pharm.* **246**:47–59 (2002).
35. P. Begat, D. A. V. Morton, J. N. Staniforth, and R. Price. The cohesive-adhesive balances in dry powder inhaler formulations I: direct quantification by atomic force microscopy. *Pharm. Res.* **21**:1591–1597 (2004).
36. C. J. Van Oss, R. J. Good, and M. K. Chaudhury. Additive and non-additive surface tension components and the interpretation of contact angles. *Langmuir* **4**:884–891 (1988).
37. R. J. Good and R. R. Stromberg. *Surface and Colloid Science*, Plenum Press, New York, 1979.
38. G. Buckton. *Interfacial Phenomena in Drug Delivery and Targeting*, Harwood Academic Publishers, Chur, Switzerland, 1995.
39. G. Buckton, P. Darcy, and D. McCarthy. The extent of errors associated with contact angles 3. The influence of surface roughness effects on angles measured using a Wilhelmy plate technique for powders. *Colloids and Surfaces A* **95**:27–35 (1995).
40. J. Schultz, L. Lavielle, and C. Martin. The role of the interface in carbon fibre-epoxy composites. *J. Adhes. Sci. Technol.* **23**:45–60 (1987).
41. V. Gutmann. *The Donor-Acceptor Approach to Molecular Interactions*, Plenum Publishing Corporation, New York, 1978.
42. F. L. Riddle and F. M. Fowkes. Spectral shifts in acid-base chemistry.1. Van der Waals contributions to acceptor numbers. *J. Am. Chem. Soc.* **112**:3259–3264 (1990).
43. N. M. Ahfat, G. Buckton, R. Burrows, and M. D. Ticehurst. Predicting mixing performance using surface energy measurements. *Int. J. Pharm.* **156**:89–95 (1997).
44. O. Planinsek, A. Trojak, and S. Srcic. The dispersive component of the surfac fee energy of powders assessed using inverse gas chromatography and contact angle measurements. *Int. J. Adhesion Adhesives* **221**:211–217 (2001).
45. J. C. Hooton, C. S. German, S. Allen, M. C. Davies, C. J. Roberts, S. J. B. Tendler, and P. M. Williams. An atomic force microscopy study of the effect of nanoscale contact geometry and surface chemistry on the adhesion of pharmaceutical particles. *Pharm. Res.* **21**:953–961 (2004).
46. J. L. Parker, D. L. Cho, and P. M. Claesson. Plasma modification of mica: forces between fluorocarbon surfaces in water and nonpolar liquid. *J. Phys. Chem.* **93**:6121–6125 (1989).
47. H. Yotsumoto and R.-H. Yoon. Application of extended DLVO theory. *J. Colloid Interface Sci.* **157**:426–433 (1993).
48. P. M. Claesson and H. K. Christenson. Very long range attractive forces between uncharged hydrocarbon and fluorocarbon surfaces in water. *J. Phys. Chem.* **92**:1650–1655 (1988).